

VIETNAM ACADEMY OF SCIENCE AND TECHNOLOGY

Vietnam Journal

of MECHANICS

Volume 36 Number 2

ISSN 0866-7136

VN INDEX 12.666

2

2014

DYNAMIC STABILITY ANALYSIS OF LAMINATED COMPOSITE PLATES WITH PIEZOELECTRIC LAYERS

Nguyen Thai Chung, Hoang Xuan Luong, Nguyen Thi Thanh Xuan*

Le Quy Don Technical University, Hanoi, Vietnam

*E-mail: nguyenthxuancdgt@yahoo.com

Received December 02, 2013

Abstract. Research on the stability to determine the critical value of structures is a complex issue but of real significance. Piezoelectric composite plate is one of the structures which have the ability to control the mechanical behaviors under loads. One of the prominent capabilities of this structure is the ability to control its vibration and stability. Using the finite element method (FEM) and construction calculation program in Matlab, the authors analyzed the elastic stability of piezoelectric composite plates under dynamic in-plane loads, taking into account damping properties of the structure. Critical loads and other factors affecting the stability of the plate are investigated.

Keywords: Piezoelectric, plate, dynamic stability, composite.

1. INTRODUCTION

Stability analysis problem of piezoelectric composite plates under static loads has attracted many researchers, but due to the complexity, the stability problem of piezoelectric composite plates under dynamic loads has less results. Alfredo R. de Faria, Mauricio V. Donadon [1], Alfredo R. de Faria [2], Dimitris Varelis, Dimitris A. Saravanos [3], Hui-Shen Shen [4], Piotr Kedziora, Aleksander Muc [5], Rajan L. Wankhade, Kamal M. Bajoria [6] investigated static stability of composite plates with piezoelectric patches by analytical methods and combined analytical methods with numerical methods. The authors investigated the effect of the position of the piezoelectric patches on the critical load of the plates. Postbuckling and vibration characteristics of piezoelectric composite plates subjected to thermopiezoelectric loads were considered by I.K. Oh, J.H. Han and I. Lee [7]. R. C Bart and T.S Geng [8] studied the stability of anisotropic plates under impact in-plane loads at the free end. With the survey size of piezoelectric patches, the authors showed the sensitivity of this factor to the stabilization of the plate. Also in this direction, by FEM method, S. Y. Wang, S.T. Quek, K.K. Ang [9] analyzed the stability of the rectangular cantilever piezoelectric composite plate, subjected to the impact in-plane loads at the free end, and used Lyapunov's stability criteria to consider stability of the plate. Stability analysis of

composite plates with piezoelectric layers under periodic in-plane loads was established by S.Pradyumna and Abhishek Gupta [10].

In the above studies, the differential vibration equations of the dynamic stability problem without damping have been solved by the integration method and critical loads were determined according to an acceptable stability criterion.

To consider the stability problems of piezoelectric composite plates, taking damping (including damping of structures and damping of piezoelectric) into account is a complex issue but closely reflects the real work of this kind of structure. Up to now, this problem has had yet a few results.

Therefore, in this paper, the authors formulate algorithms, calculating programs and research on critical loads of piezoelectric composite plates with any type of dynamic loads acting on the plane of the plate, including the damping of structures.

2. FINITE ELEMENT FORMULATION AND THE GOVERNING EQUATIONS

Consider laminated composite plates with general coordinate system (x, y, z) , in which the x, y plane coincides with the neutral plane of the plate. The top surface and lower surface of the plate are bonded to the piezoelectric patches or piezoelectric layers (actuator and sensor). The plate under the load acting on its neutral plane has any temporal variation rule (Fig. 1).

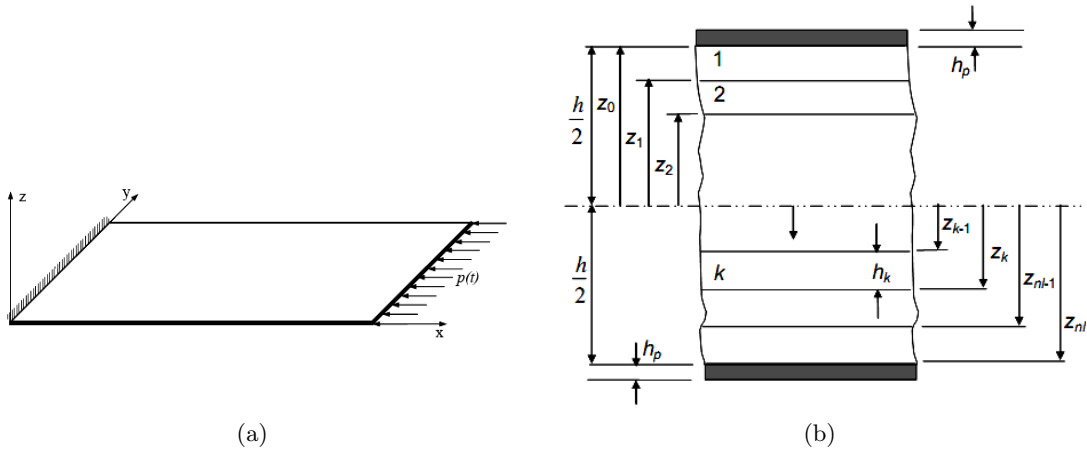


Fig. 1. Piezoelectric composite plate and coordinate system of the plate (a), and Lamina details (b)

Hypothesis: The piezoelectric composite plate corresponds with Reissner-Mindlin theory. The material layers are arranged symmetrically through the neutral plane of the plate, ideally adhesive with each other. The authors use FEM to establish equations and formulate the algorithm, calculation program. The homogenization methods to calculate the composite plate are also used.

2.1. Strain-displacement relations

Based on the first-order shear deformation theory, the displacement fields at any point in the plate are [11, 12]

$$\begin{aligned} u(x, y, z, t) &= u_0(x, y, t) + z\theta_y(x, y, t), \\ v(x, y, z, t) &= v_0(x, y, t) - z\theta_x(x, y, t), \\ w(x, y, z, t) &= w_0(x, y, t), \end{aligned} \quad (1)$$

where u, v and w are the displacements of a general point (x, y, z) in the laminate along x, y and z directions, respectively. u_0, v_0, w_0, θ_x and θ_y are the displacements and rotations of a midplane transverse normal about the y - and x -axes respectively.

The components of the strain vector corresponding to the displacement field (1) are [11, 13]. For the linear strain

$$\begin{aligned} \varepsilon_x &= \frac{\partial u}{\partial x} = \frac{\partial u_0}{\partial x} + z\frac{\partial \theta_y}{\partial x}, \quad \varepsilon_y = \frac{\partial v}{\partial y} = \frac{\partial v_0}{\partial y} - z\frac{\partial \theta_x}{\partial y}, \\ \gamma_{xy} &= \left(\frac{\partial u}{\partial y} + \frac{\partial v}{\partial x} \right) + \frac{\partial w}{\partial x} \cdot \frac{\partial w}{\partial y} = \left(\frac{\partial u_0}{\partial y} + \frac{\partial v_0}{\partial x} \right) + z \left(\frac{\partial \theta_y}{\partial x} - \frac{\partial \theta_x}{\partial y} \right), \\ \gamma_{xz} &= \frac{\partial u}{\partial z} + \frac{\partial w}{\partial x} = \frac{\partial w_0}{\partial x} + \theta_y, \quad \gamma_{yz} = \frac{\partial v}{\partial z} + \frac{\partial w}{\partial y} = \frac{\partial w_0}{\partial y} - \theta_x, \end{aligned} \quad (2)$$

or in vector form

$$\begin{aligned} \begin{Bmatrix} \varepsilon_x \\ \varepsilon_y \\ \gamma_{xy} \end{Bmatrix} &= \begin{Bmatrix} \varepsilon_x^0 \\ \varepsilon_y^0 \\ \gamma_{xy}^0 \end{Bmatrix} + z \begin{Bmatrix} \kappa_x \\ \kappa_y \\ \kappa_{xy} \end{Bmatrix} = \begin{bmatrix} \frac{\partial}{\partial x} & 0 \\ 0 & \frac{\partial}{\partial y} \\ \frac{\partial}{\partial y} & \frac{\partial}{\partial x} \end{bmatrix} \begin{Bmatrix} u_0 \\ v_0 \end{Bmatrix} + z \begin{bmatrix} -\frac{\partial}{\partial y} & 0 \\ 0 & -\frac{\partial}{\partial x} \\ -\frac{\partial}{\partial y} & \frac{\partial}{\partial x} \end{bmatrix} \begin{Bmatrix} \theta_x \\ \theta_y \end{Bmatrix} \\ &= [D_\varepsilon] \begin{Bmatrix} u_0 \\ v_0 \end{Bmatrix} + [D_\kappa] \begin{Bmatrix} \theta_x \\ \theta_y \end{Bmatrix} = \{\varepsilon_0\} + z\{\kappa\} = \{\varepsilon_b^L\}, \end{aligned} \quad (3a)$$

$$\begin{Bmatrix} \gamma_{xz} \\ \gamma_{yz} \end{Bmatrix} = \begin{bmatrix} \frac{\partial}{\partial x} & 0 & 1 \\ \frac{\partial}{\partial y} & -1 & 0 \end{bmatrix} \begin{Bmatrix} w^0 \\ \theta_x \\ \theta_y \end{Bmatrix} = [{}^wD] \begin{Bmatrix} w_0 \\ \theta_x \\ \theta_y \end{Bmatrix} = \{\varepsilon_s\} \quad (3b)$$

and for the nonlinear strain

$$\begin{Bmatrix} \varepsilon_x \\ \varepsilon_y \\ \gamma_{xy} \end{Bmatrix} = \{\varepsilon_b^L\} + \{\varepsilon^N\} = \{\varepsilon_b^N\} \quad (4a)$$

$$\begin{Bmatrix} \gamma_{xz} \\ \gamma_{yz} \end{Bmatrix} = \{\varepsilon_s\}, \quad (4b)$$

where $\{\varepsilon^N\} = \frac{1}{2} \begin{bmatrix} \frac{\partial w_0}{\partial x} & 0 \\ 0 & \frac{\partial w_0}{\partial y} \\ \frac{\partial w_0}{\partial y} & \frac{\partial w_0}{\partial x} \end{bmatrix} \begin{Bmatrix} \frac{\partial}{\partial x} \\ \frac{\partial}{\partial y} \end{Bmatrix} w_0$ is the non-linear strain vector, $\{\varepsilon_b^L\}$ is the linear strain vector, $\{\varepsilon_s\}$ is the shear strain vector.

2.2. Stress-strain relations

The equation system describing the stress-strain relations and mechanical-electrical quantities is respectively written as follows [10, 14]

$$\{\sigma_b\} = [Q] \{\varepsilon_b^N\} - [e] \{E\}, \quad \{\tau_b\} = [Q_s] \{\varepsilon_s\}, \quad (5)$$

$$\{D\} = [e] \{\varepsilon_b^N\} + [p] \{E\}, \quad (6)$$

where $\{\sigma_b\} = \{\sigma_x \ \sigma_y \ \tau_{xy}\}^T$ is the plane stress vector, $\{\tau_b\} = \{\tau_{yz} \ \tau_{xz}\}^T$ is the shear stress vector, $[Q]$ is the ply in-plane stiffness coefficient matrix in the structural coordinate system, $[Q_s]$ is the ply out-of-plane shear stiffness coefficient matrix in the structural coordinate system [14], $[e]$ is the piezoelectric stress coefficient matrix, $[p]$ is the permittivity coefficient matrix, $\{E_k\} = \{E_k^x \ E_k^y \ E_k^z\}^T$ is the electric-field vector. If the voltage is applied to the actuator in the thickness only, then $\{E_k\} = \{0 \ 0 \ -\frac{V_k}{t_k}\}^T$, V_k is the applied voltage across the k^{th} ply, and t_k is the thickness of the k^{th} piezoelectric layer. Notice that $\{\tau_b\}$ is free from piezoelectric effects [15].

The in-plane force vector at the state pre-buckling

$$\{N^0\} = \{N_x^0 \ N_y^0 \ N_{xy}^0\}^T = \sum_{k=1}^n \int_{h_{k-1}}^{h_k} \left\{ \begin{array}{c} \sigma_x^0 \\ \sigma_y^0 \\ \tau_{xy}^0 \end{array} \right\}_k dz. \quad (7)$$

2.3. Total potential energy

The total potential energy of the system is given by [9, 16]

$$\Pi = \frac{1}{2} \int_{V_p} \{\varepsilon_b^N\}^T \{\sigma_b\} dV + \frac{1}{2} \int_{V_p} \{\varepsilon_s\}^T \{\tau_b\} dV - \frac{1}{2} \int_{V_p} \{E\}^T \{D\} dV - W, \quad (8)$$

where W is the energy of external forces, V_p is the entire domain including composite and piezoelectric materials.

Introducing $[A]$, $[B]$, $[D]$, $[A_s]$ and vectors $\{N_p\}$, $\{M_p\}$ as

$$([A], [B], [D]) = \int_{-h/2}^{h/2} (1, z, z^2) [Q] dz, [A_s] = \int_{-h/2}^{h/2} [Q_s] dz, (\{N_p\}, \{M_p\}) = \int_{-h/2}^{h/2} (1, z) [e] \{E\} dz, \quad (9)$$

where h is the total laminated thickness and combining with (5), (6) the total potential energy equation (8) can be written

$$\begin{aligned} \Pi = & \frac{1}{2} \int_{\Omega} \{\varepsilon_0\}^T [A] \{\varepsilon_0\} d\Omega + \frac{1}{2} \int_{\Omega} \{\kappa\}^T [D] \{\kappa\} d\Omega + \frac{1}{2} \int_{\Omega} \{\varepsilon_s\}^T [A_s] \{\varepsilon_s\} d\Omega + \\ & + \int_{\Omega} \{\varepsilon^N\}^T ([A] \{\varepsilon_0\} - [N_p]) d\Omega - \int_{\Omega} \{\varepsilon_0\}^T [N_p] d\Omega - \int_{\Omega} \{\kappa\}^T [M_p] d\Omega - W, \end{aligned} \quad (10)$$

where Ω is the plane xy domain of the plate.

2.4. Finite element models

Nine-node Lagrangian finite elements are used with the displacement and strain fields represented by Eqs. (1) and (4). In the developed models, there is one electric potential degree of freedom for each piezoelectric layer to represent the piezoelectric behavior and thus the vector of electrical degrees of freedom is [6]

$$\{\phi^e\} = \{ \cdot \cdot \phi_j^e \cdot \cdot \}^T, \quad j = 1, \dots, \text{NPL}^e, \quad (11)$$

where NPL^e is the number of piezoelectric layers in a given element.

The vector of degrees of freedom for the element $\{q^e\}$ is

$$\{q^e\} = \{ \{q_1^e\} \quad \{q_2^e\} \quad \dots \quad \{q_9^e\} \quad \phi^e \}^T, \quad (12)$$

where $\{q_i^e\} = \{u_i \quad v_i \quad w_i \quad \theta_{x_i} \quad \theta_{y_i}\}^T$ is the mechanical displacement vector for node i .

From Eqs. (3a), (3b), we receive

$$\{\varepsilon\} = [B_b] \{q\}. \quad (13)$$

2.5. Dynamic equations

The dynamic equations of piezoelectric composite plate can be derived by using Hamilton's principle [11]

$$\delta \int_{t_1}^{t_2} [T - \Pi] dt = 0, \quad (14)$$

where T is the kinetic energy.

The kinetic energy at the element level is defined as

$$T^e = \frac{1}{2} \int_{V_e} \rho \{\dot{q}^e\}^T \{\dot{q}^e\} dV_e. \quad (15)$$

The energy of external forces for an element

$$W^e = \int_{V_e} \{q^e\}^T \{f_b\} dV_e + \int_{S_e} \{q^e\}^T \{f_s\} dS_e + \{q^e\}^T \{f_c\}, \quad (16)$$

where V_e is the volume of the plate elements, $\{f_b\}$ is the body force vector, S_e is the surface area of the plate elements, $\{f_s\}$ is the surface force and $\{f_c\}$ is the concentrated load.

The total kinetic energy

$$T = \frac{1}{2} \sum_{Ne} \int_{V_e} \rho \{\dot{q}^e\}^T \{\dot{q}^e\} dV_e. \quad (17)$$

The total energy of external forces for an element

$$W = \sum_{Ne} \left(\int_{V_e} \{q^e\}^T \{f_b\} dV_e + \int_{S_e} \{q^e\}^T \{f_s\} dS_e + \{q^e\}^T \{f_c\} \right), \quad (18)$$

where Ne is the number of the elements.

Substituting Eqs. (10), (17) and (18) into Eq. (14) and using Eq. (13), the dynamic matrix equations can be written as

The vibration equation of the membrane (without damping) with in-plane loads is [11]

$$[M_{ss}] \{\ddot{q}_{ss}\} + [K_{ss}] \{q_{ss}\} = \{F(t)\}, \quad (19)$$

The equation of bending vibrations with out-of-plane loads is

$$\begin{bmatrix} [M_{bb}] & [0] \\ [0] & [0] \end{bmatrix} \begin{Bmatrix} \{\ddot{q}_{bb}\} \\ \{\dot{\phi}\} \end{Bmatrix} + \begin{bmatrix} [C_R] & [0] \\ [0] & [0] \end{bmatrix} \begin{Bmatrix} \{\dot{q}_{bb}\} \\ \{\dot{\phi}\} \end{Bmatrix} + \begin{bmatrix} [K_{bb}] + [K_G] & [K_{b\phi}] \\ [K_{\phi b}] & -[K_{\phi\phi}] \end{bmatrix} \begin{Bmatrix} \{q_{bb}\} \\ \{\phi\} \end{Bmatrix} = \begin{Bmatrix} \{R\} \\ \{Q_{el}\} \end{Bmatrix}, \quad (20)$$

where $[M_{ss}], [K_{ss}]$ and $\{q_{ss}\}, \{\dot{q}_{ss}\}, \{\ddot{q}_{ss}\}$ are the overall mass, membrane elastic stiffness matrix and the membrane displacement, velocity, acceleration vector; $[C_R] = \alpha_R [M_{bb}] + \beta_R [K_{bb}]$ is the overall structural damping matrix (where α_R, β_R are the damping coefficients, which are generally determined by the first and second natural frequencies and ratio of damping ξ); $[M_{bb}], [K_{bb}]$ and $\{q_{bb}\}, \{\dot{q}_{bb}\}, \{\ddot{q}_{bb}\}$ are the overall mass, bending elastic stiffness matrix and the bending displacement, velocity, acceleration vector; $[K_G]$ is the overall geometric stiffness matrix ($[K_G]$ is a function of external in-plane loads); $[K_{b\phi}]$ is the overall coupling matrices between elastic mechanical and electrical effects; $[K_{\phi b}]$ is the overall coupling matrices between electrical and elastic mechanical effects; $[K_{\phi\phi}]$ is the overall dielectric “stiffness” matrix [1, 3, 12]; $\{\phi\}$ is the overall electric potential vector; $\{F(t)\}$ is the in-plane load vector, $\{R\}$ is the normal load vector, $\{Q_{el}\}$ is the vector containing the nodal charges and in-balance charges. The element coefficient matrices are [8, 11, 15]

$$[M_{bb}^e] = \int_{V_e} \rho [N_i]^T [m] [N_i] dV_e, [M_{ss}^e] = \int_{V_e} \rho [N_i^s]^T [m] [N_i^s] dV_e, [K_{\phi\phi}^e] = - \int_{V_e} [B_\phi]^T [p] [B_\phi] dV_e,$$

$$[K_{b\phi}^e] = \int_{V_e} [B_b]^T [e] [B_\phi] dV_e, [K_{\phi\phi}^e] = \sum_{NPe} [K_{\phi\phi}^e], [K_{b\phi}] = \sum_{NPe} [K_{b\phi}^e], [K_{\phi b}] = [K_{b\phi}]^T,$$

where $[N_i]$ is the shape functions in case of bending plate, $[N_i]$ is the shape functions in case of tensile or compression plate, NPe is the number of the piezoelectric composite plate elements, $[B_\phi]$ is the matrix relating the electric potential.

$[K_G^e] = [K_{Gx}^e] + [K_{Gy}^e] + [K_{Gxy}^e]$ is the element geometric stiffness matrix, with the components identified

$$\begin{aligned} [K_{Gx}^e] &= \int_{A_e} N_x^0 [N'_x] [N'_x]^T dA_e, \\ [K_{Gy}^e] &= \int_{A_e} N_y^0 [N'_y] [N'_y]^T dA_e, \\ [K_{Gxy}^e] &= \int_{A_e} N_{xy}^0 [N'_x] [N'_y]^T dA_e, \end{aligned} \quad (21)$$

where

$$[N'_x] = \frac{\partial}{\partial x} [N(x, y)], [N'_y] = \frac{\partial}{\partial y} [N(x, y)], \quad (22)$$

$$\frac{\partial w}{\partial x} = \left[\frac{\partial N}{\partial x} \right] \{q_{bb}^e\} = [N'_x] \{q_{bb}^e\}, \quad \frac{\partial w}{\partial y} = \left[\frac{\partial N}{\partial y} \right] \{q_{bb}^e\} = [N'_y] \{q_{bb}^e\}. \quad (23)$$

$$[K_G] = \sum_{ne} [K_G^e]. \quad (24)$$

3. DYNAMIC STABILITY ANALYSIS

When the plate is subjected to in-plane loads only ($\{R\} = \{0\}$), the in-plane stresses can lead to buckling, from Eqs. (19) and (20) the governing differential equations of motion of the damped system may be written as

$$[M_{ss}] \{\ddot{q}_{ss}\} + [K_{ss}] \{q_{ss}\} = \{F(t)\}, \quad (25a)$$

$$[M_{bb}] \{\ddot{q}_{bb}\} + [C_R] \{\dot{q}_{bb}\} + ([K_{bb}] + [K_G]) \{q_{bb}\} + [K_{b\phi}] \{\phi\} = \{0\}, \quad (25b)$$

$$[K_{\phi b}] \{q_{bb}\} - [K_{\phi\phi}] \{\phi\} = \{Q_{el}\}. \quad (25c)$$

Substituting $\{\phi\}$ from (25c) into (25b), yields

$$[M_{bb}] \{\ddot{q}_{bb}\} + [C_R] \{\dot{q}_{bb}\} + \left([K_{bb}] + [K_{b\phi}] [K_{\phi\phi}]^{-1} [K_{\phi b}] + [K_G] \right) \{q_{bb}\} = [K_{b\phi}] [K_{\phi\phi}]^{-1} \{Q_{el}\} \quad (26)$$

Plate vibrations induce charges and electric potentials in sensor layers. The control system allows a current to flow and feeds this back to the actuators. Note that, due to the absolute adhesion of the piezoelectric layers (patches) to the surface of the plate, they should have the same mechanical displacement with the plate. Therefore, $\{u\}_a = \{u\}_s = \{q_{bb}\}$, $\{\dot{u}\}_a = \{\dot{u}\}_s = \{\dot{q}_{bb}\}$ (where $\{u\}_a$ is the actuator displacement vector, $\{u\}_s$ is the sensor displacement vector. If no external charge Q_{el} is applied to a sensor, from (25c) we have

$$\{\phi\} = \{\phi_s\} = \left[K_{\phi\phi}^{-1} \right]_s [K_{\phi b}]_s \{u\}_s, \quad (27)$$

is the generated potential in sensor. $\{Q_{el}\}_s = [K_{\phi b}]_s \{u\}_s$ is the induced charge due to the deformation.

The operation of the amplified control loop implying the actuating voltage is

$$\{\phi\}_a = G_d \{\phi\}_s + G_v \left\{ \dot{\phi} \right\}_s, \quad (28)$$

where G_d and G_v are the feedback control gains for displacement and velocity, respectively.

From (25c) and (28), the charge in the actuator deformation in response to plate vibration modified by control system feedback is

$$\{Q_{el}\}_a = [K_{\phi b}]_a \{u\}_a - [K_{\phi\phi}]_a \{\phi\}_a = [K_{\phi b}]_a \{u\}_a - [K_{\phi\phi}]_a \left(G_d \{\phi\}_s + G_v \left\{ \dot{\phi} \right\}_s \right) \quad (29)$$

Substituting (27) into (29), yields

$$\{Q_{el}\}_a = [K_{\phi b}]_a \{u\}_a - G_d [K_{\phi\phi}]_a \left[K_{\phi\phi}^{-1} \right]_s [K_{\phi b}]_s \{u\}_s - G_v [K_{\phi\phi}]_a \left[K_{\phi\phi}^{-1} \right]_s [K_{\phi b}]_s \{\dot{u}\}_s \quad (30)$$

Then substitution of (30) into (26), leads to

$$\begin{aligned} & [M_{bb}] \{\ddot{q}_{bb}\} + [C_R] \{\dot{q}_{bb}\} + \left([K_{bb}] + [K_{b\phi}] [K_{\phi\phi}]^{-1} [K_{\phi b}] + [K_G] \right) \{q_{bb}\} = \\ & = [K_{b\phi}] [K_{\phi\phi}]^{-1} \left([K_{\phi b}]_a \{u\}_a - G_d [K_{\phi\phi}]_a [K_{\phi\phi}^{-1}]_s [K_{\phi b}]_s \{u\}_s - G_v [K_{\phi\phi}]_a [K_{\phi\phi}^{-1}]_s [K_{\phi b}]_s \{\dot{u}\}_s \right). \end{aligned} \quad (31)$$

Due to the absolute adhesion between the piezoelectric layer with the plate surface, so

$$[K_{b\phi}]_a \equiv [K_{b\phi}]_s \equiv [K_{b\phi}], \quad [K_{\phi\phi}]_a \equiv [K_{\phi\phi}]_s \equiv [K_{\phi\phi}].$$

Eq. (31) is rewritten as

$$\begin{aligned} & [M_{bb}] \{\ddot{q}_{bb}\} + \left([C_R] \{\dot{q}_{bb}\} + G_v [K_{\phi\phi}] [K_{\phi\phi}^{-1}] [K_{\phi b}] \right) \{\dot{q}_{bb}\} + \\ & + \left([K_{bb}] + G_d [K_{b\phi}] [K_{\phi\phi}]^{-1} [K_{\phi\phi}] [K_{\phi\phi}^{-1}] [K_{\phi b}] + [K_G] \right) \{q_{bb}\} = \{0\}, \end{aligned} \quad (32)$$

or

$$[M_{bb}] \{\ddot{q}_{bb}\} + ([C_R] + [C_A]) \{\dot{q}_{bb}\} + ([K^*] + [K_G]) \{q_{bb}\} = \{0\}, \quad (33)$$

where $[C_A] = G_v [K_{\phi\phi}] [K_{\phi\phi}^{-1}] [K_{\phi b}]$ is the overall active damping matrix; $[C_R] = \alpha_R [M_{bb}] + \beta_R [K_{bb}]$ is the overall structural damping matrix; $[K^*] = [K_{bb}] + G_d [K_{b\phi}] [K_{\phi\phi}]^{-1} [K_{\phi\phi}] [K_{\phi\phi}^{-1}] [K_{\phi b}]$ is the overall active stiffness matrix.

Combining (25a) and (33), we obtain the stability equations of the laminated composite plates with piezoelectric layers

$$\begin{cases} [M_{ss}] \{\ddot{q}_{ss}\} + [K_{ss}] \{q_{ss}\} = \{F(t)\}, & (34a) \\ [M_{bb}] \{\ddot{q}_{bb}\} + ([C_A] + [C_R]) \{\dot{q}_{bb}\} + ([K^*] + [K_G]) \{q_{bb}\} = \{0\}. & (34b) \end{cases}$$

The overall geometric stiffness matrix K_G is defined as follows

- In case of only tensile or compression plates ($w_e = 0$): Solving the Eq. (34a) helps us to present unknown displacement vector $\{q_{ss}\}$, and then stress vector

$$\{\sigma_{ss}\} = [A_s] [B_s] \{q_{ss}\}, \quad (35)$$

where $[A_s]$ and $[B_s]$ are the stiffness coefficient matrix and strain-displacement matrix of the plane problem [11].

Membrane force vector $\{N^0\}$ is defined by (7) and $[K_G]$ is defined by (21) and (24).

- In case of bending plate ($w_e \neq 0$): The stress vector is

$$\{\sigma_{sb}\} = \{\sigma_{ss}\} + \{\sigma_{bb}\}, \quad (36)$$

$$\{\sigma_{bb}\} = [A_b] [B_b] \{q_{bb}\},$$

where $[A_b]$ and $[B_b]$ are the stiffness coefficient matrix and strain-displacement matrix of the plane bending problem [11]), membrane force vector $\{N^0\}$ is defined by (7) and $[K_G]$ is defined by (21) and (24).

Stability criteria [8, 10]:

• In case of the plate under periodic in-plane loads and without damping, the elastic stability problems become simple only by solving the linear equations to determine the eigenvalues [10].

• In case of the plate under any in-plane dynamic load and with damping, the elastic stability problems become very complex. This iterative method can be proved effectively and the following dynamic stability criteria are used [8].

- Plate is considered to be stable if the maximum bending deflection is three times smaller than the plate's thickness: Eq. (34b) has the solution $(w_i)_{max}$ satisfying the condition $0 \leq |w_i|_{max} < 3h$, where w_i is the deflection of the plate at node number i .

- Plate is called to be in critical status if the maximum bending deflection of the plate is three times equal to the plate's thickness. Eq. (34b) has the solution $(w_i)_{max}$ satisfying the condition $|w_i|_{max} = 3h$.

- Plate is called to be at buckling if the maximum deflection of the plate is three times larger than the plate's thickness: Eq. (34b) has the solution $(w_i)_{max}$ satisfying the condition $|w_i|_{max} > 3h$.

The identification of critical forces is carried out by the iterative method.

4. ITERATIVE ALGORITHM

Step 1. Defining the matrices, the external load vector and errors of load iterations

Step 2. Solving the Eq. (34a) to present unknown displacement vector, $\{q_{ss}\}$ and the stress vector is defined by (35), updating the geometric stiffness matrix $[K_G]$.

Step 3. Solving the Eq. (34b) to present unknown bending displacement vector $\{q_{bb}\}$, and then testing stability conditions

- If for all $|w_i| = 0$: increase load, recalculate from step 2;

- If at least one value $|w_i| \neq 0$:

+ In case: $0 < |w_i|_{max} < 3h$: Define stress vector by Eq. (36), update the geometric stiffness matrix $[K_G]$. Increase load, recalculate from step 2;

+ In case: $0 \leq \frac{|w_i|_{max} - 3h}{|w_i|_{max}} \leq \varepsilon_D$: Critical load $p = p_{cr}$. End.

5. NUMERICAL APPLICATIONS

5.1. Validation of numerical code and comparison

For the validation of the Matlab code developed for the finite element analysis of the piezoelectric composite plate, we resolve the elastic dynamic buckling problem of S.Pradyumna and Abhishek Gupta [10] by the present algorithm and compare the results obtained with the published results. Square plate edges $a = 24$ mm, layer layout rules (P/0⁰/90⁰/90⁰/0⁰/P), the total thickness of the plate $h = 1$ mm, each composite layer is made of the graphite-epoxy material and the thickness is $0.2h$, each piezoelectric layer thickness $h_p = 0.1h$ is PZT-5A. The plate under periodic in-plane load ($P(t) = \alpha P_{cr} + \beta P_{cr} \cos \bar{\Omega}t$) is evenly distributed on two opposite edges of the plate, where α and β are static and dynamic load factors, respectively; P_{cr} is the static elastic buckling load of the plate; $\bar{\Omega}$ is the excitation frequency. Material properties for Graphite-Epoxy orthotropic layer are $E_1 = 150$ GPa, $E_2 = 9$ GPa, $G_{12} = G_{13} = 7.1$ GPa, $G_{23} = 2.5$ GPa, $\nu_{12} = \nu_{23} = \nu_{32} = 0.3$, $\rho_{GE} = 1580$ kg/m³ and for PZT-5A piezoelectric layer $E = 63.0$ GPa, $G = 24.2$ GPa, $\nu = 0.3$, $\rho_{pzt} = 7600$ kg/m³, $d_{31} = d_{32} = 2.54 \times 10^{-10}$ m/V.

Consider the case with nondimensional excitation frequency ($\Omega = \bar{\Omega}/\omega_1$), where ω_1 is the first natural frequency of the plate and $\alpha = 0$, voltage at the top and bottom piezoelectric layers is $V = 100$ V. The comparison of results on dynamic instability regions of the plate is shown in Fig. 2.

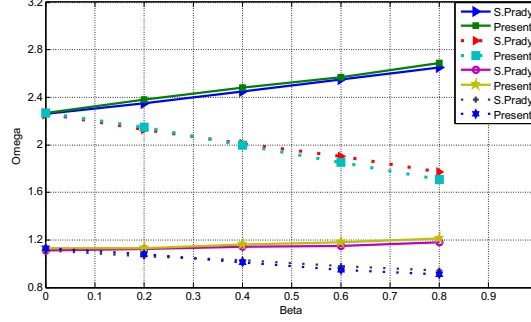


Fig. 2. Comparison on dynamic instability regions of the plate ((P/0⁰/90⁰/90⁰/0⁰/P), $a = b = 24$ mm, $h = 1$ mm, $h_p = 0.1$ mm, $\alpha = 0$, $V = 100$ V)

In this case, it is shown that the results obtained in this research are in good agreement with those of the published papers [15] the errors are very small (the maximum error value is 0.206%).

5.2. Numerical results

Stability analysis of piezoelectric composite plate with dimensions $a \times b \times h$, where $a = 0.25$ m, $b = 0.30$ m, $h = 0.002$ m. Piezoelectric composite plate is composed of 3 layers, in which two layers of piezoelectric PZT-5A at its top and bottom are considered, each layer thickness $h_p = 0.00075$ m; the middle layer material is Graphite/Epoxy material, with thickness $h_1 = 0.0005$ m. The material properties for graphite/epoxy and PZT-5A are shown in section 5.1 above. One short edge of the plate is clamped, the other three edges are free. The in-plane half-sine load is evenly distributed on the short edge of the plate: $p(t) = p_0 \sin(2\pi ft)$, where p_0 is the amplitude of load, $f = 1/T = 1/0.01 = 100$ Hz ($0 \leq t \leq T/2 = 0.005$ s) is the excitation frequency, voltage applied $V = 50$ V. The iterative error of the load $\varepsilon_D = 0.02\%$ is chosen.

5.2.1. Effect of the damping

Consider two cases: with damping ($\xi = 0.05$, $G_v = 0.5$, $G_d = 15$) and without damping ($\xi = 0.0$, $G_v = 0.0$, $G_d = 15$).

The response of vertical displacement at the plate centroid over the plate thickness for the two cases is shown in Fig. 3.

The results show that the critical load of the plate with damping is larger than that without damping. In the two cases above, the critical load rises by 6.8%.

5.2.2. Effect of the applied voltages

Analyze the stability of the plate with damping when a voltage of -200, -150, -100, -50, 0, 50, 100, 150 and 200V is applied to the actuator layer of the piezoelectric composite plate.

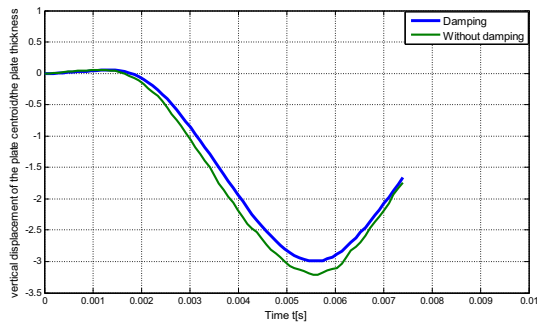


Fig. 3. Time history of the vertical displacement at the plate centroid over the plate thickness

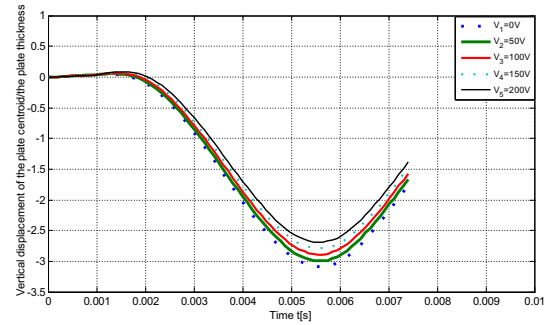


Fig. 4. Time history of the vertical displacement at the plate centroid over the plate thickness

Fig. 4 shows the time history of the vertical displacement at the plate centroid over the plate thickness when a voltage of 0, 50, 100, 150 and 200V is applied.

The relation between critical load and voltages is shown in Fig. 5. The results show that the voltage applied to the piezoelectric layers affects the stability of the plate. As the voltage increases, the critical load of the plate also increases.

5.2.3. Effect of the amplitude of the load

When the amplitude of the load changes from 0.25pcr to 1.5pcr (where pcr is the amplitude of the critical load), a voltage of 50V is applied to the actuator layer of the plate.

The results show the time history response of the vertical displacement at the plate centroid over the plate thickness as seen in Fig. 6, $p_0 = 0.25p_{cr}, 0.5p_{cr}, 0.75p_{cr}, 1.0p_{cr}, 1.25p_{cr}, 1.5p_{cr}$.

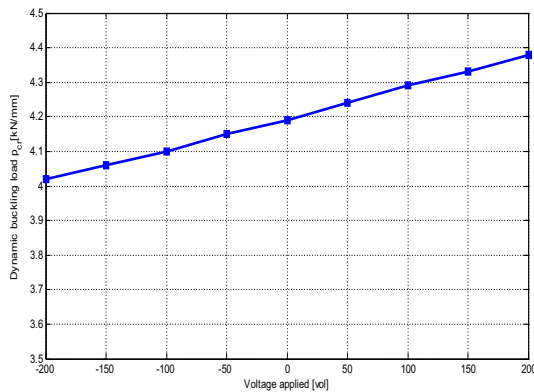


Fig. 5. Critical load-voltage relation

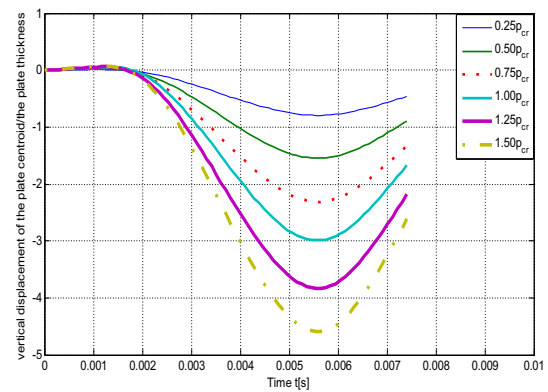


Fig. 6. Time history of the vertical displacement at the plate centroid over the plate thickness

From Fig. 6 as can see that when the amplitude of the load acting on the plane of plate increases, the plate is buckled early.

6. CONCLUSIONS

The differential vibration equations, algorithms and program of linear stability analysis of piezoelectric composite plates under any dynamic load in the plane of the plate taking into account structural damping and piezoelectric damping have been formulated.

The validation of the present formulation is carried out that provides the accuracy of the choosing research method. The obtained results show:

- In case with damping, the critical load of the plate is higher than that without damping. In case with damping, the plate is buckled later than that without damping.

- When the voltage applied to the actuator layer of the piezoelectric composite plate increases, the critical load of the plate increases.

REFERENCES

- [1] A. R. d. Faria and M. V. Donadon. The use of piezoelectric stress stiffening to enhance buckling of laminated plates. *Latin American Journal of Solids and Structures*, **7**, (2), (2010), pp. 167–183.
- [2] A. R. de Faria. Buckling optimization and prebuckling enhancement of imperfect composite plates using piezoelectric actuators. In *2th International Conference on Engineering Optimization*, Lisbon, Portugal, (September 6-9, 2010). pp. 1–16.
- [3] D. Varelis and D. A. Saravanos. Coupled buckling and postbuckling analysis of active laminated piezoelectric composite plates. *International Journal of Solids and Structures*, **41**, (5), (2004), pp. 1519–1538.
- [4] H.-S. Shen. Postbuckling of shear deformable laminated plates with piezoelectric actuators under complex loading conditions. *International Journal of Solids and Structures*, **38**, (44), (2001), pp. 7703–7721.
- [5] P. Kedziora and A. Muc. Stability of piezoelectric circular plates. *Mechanics and Mechanical Engineering*, **14**, (2), (2010), pp. 223–232.
- [6] R. L. Wankhade and K. M. Bajoria. Stability of simply supported smart piezolaminated composite plates using finite element method. In *Proceeding of the International Conference on Advances in Aeronautical and Mechanical Engineering-AME*, (2012), pp. 14–19.
- [7] I.-K. Oh, J.-H. Han, and I. Lee. Postbuckling and vibration characteristics of piezolaminated composite plate subject to thermopiezoelectric loads. *Department of Aerospace Engineering, Korea Advanced Institute of Science and Technology*, (2000).
- [8] R. Batra and T. Geng. Enhancement of the dynamic buckling load for a plate by using piezoceramic actuators. *Smart Materials and Structures*, **10**, (5), (2001), pp. 925–933.
- [9] S. Wang, S. Quek, and K. Ang. Dynamic stability analysis of finite element modeling of piezoelectric composite plates. *International Journal of Solids and Structures*, **41**, (3), (2004), pp. 745–764.
- [10] S. Pradyumna and A. Gupta. Dynamic stability of laminated composite plates with piezoelectric layers subjected to periodic in-plane load. *International Journal of Structural Stability and Dynamics*, **11**, (2), (2011), pp. 297–311.
- [11] O. Zienkiewicz and R. Taylor. *The finite element method*. McGraw-Hill, International Edition, (1998).

- [12] T. I. Thinh and L. K. Ngoc. Static and dynamic analysis of laminated composite plates with integrated piezoelectric. *Vietnam Journal of Mechanics, VAST*, **30**, (1), (2008), pp. 55–66.
- [13] N. T. Chung, P. T. Dat, and B. T. Cuong. Geometrical nonlinear elastic buckling of the composite cylindrical shell. In *Proceeding of the International Conference on Computational Solid Mechanics*, (2008), pp. 67–76.
- [14] J. N. Reddy. *Mechanics of laminated composite plates and shells: theory and analysis*. CRC press, (2003).
- [15] M. Kögl and M. Bucalem. A family of piezoelectric mitc plate elements. *Computers & structures*, **83**, (15), (2005), pp. 1277–1297.
- [16] R. L. Wankhade and K. M. Bajoria. Buckling analysis of piezolaminated plates using higher order shear deformation theory. *International Journal of Composite Materials*, **3**, (4), (2013), pp. 92–99.

CONTENTS

	Pages
1. Dao Huy Bich, Nguyen Dang Bich, A coupling successive approximation method for solving Duffing equation and its application.	77
2. Nguyen Thai Chung, Hoang Xuan Luong, Nguyen Thi Thanh Xuan, Dynamic stability analysis of laminated composite plate with piezoelectric layers.	95
3. Vu Le Huy, Shoji Kamiya, A direct evidence of fatigue damage growth inside silicon MEMS structures obtained with EBIC technique.	109
4. Nguyen Tien Khiem, Duong The Hung, Vu Thi An Ninh, Multiple crack identification in stepped beam by measurements of natural frequencies.	119
5. Nguyen Hong Son, Hoang Thi Bich Ngoc, Dinh Van Phong, Nguyen Manh Hung, Experiments and numerical calculation to determine aerodynamic characteristics of flows around 3D wings.	133
6. Gulshan Taj M. N. A., Anupam Chakrabarti, Mohammad Talha, Free vibration analysis of four parameter functionally graded plate accounting for realistic transverse shear mode.	145